

# Nuclear magnetic resonance approach to fractal chain structure in molten polymers and gels: Characterization method of the spin-system response

J. P. Cohen-Addad and C. Schmit

*Laboratoire de Spectrométrie Physique associé au CNRS, Université Scientifique, Technologique et Médicale de Grenoble, BP 87, 38402 St Martin d'Hères Cédex, France*  
(Received 21 April 1987; accepted 30 November 1987)

By observing protons attached to polymer chains, pulse sequences are proposed to disclose transverse magnetization properties specific to polymer network structures. It is shown that a peculiar relaxational behaviour originates from the existence of a residual energy  $\hbar\Delta_r$ , of spin-spin interactions closely associated with the existence of chain coupling junctions. Properties are illustrated by observing vulcanized polybutadiene and polyethylene, at room temperature and 418 K, respectively. Furthermore, it is shown that these properties are clearly modified when coupling junctions in a melt fluctuate within time intervals shorter than  $\Delta_r^{-1}$ . Finally, a pulse sequence is proposed to eliminate both the residual energy and diamagnetic inhomogeneities occurring in most polymeric systems. This elimination thus reveals effects of monomeric-unit high-frequency motions.

(Keywords: polybutadiene; polyethylene; crosslinks; entanglements; nuclear magnetic resonance)

## INTRODUCTION

One of the main problems encountered in describing the low-frequency behaviour of a polymer melt or the static mechanical response of a polymeric gel, whether mineral-filled or not, is the difficulty of probing individual statistical properties of elementary chain segments; these are known to govern basic viscoelastic effects in these systems<sup>1,2</sup>. Elementary chains are usually determined from temporary junctions in a melt (entanglements), while they have permanently fixed end-points, at least on average, in a gel (crosslinks or trapped entanglements)<sup>3,4</sup>. The statistical volume  $V_c$  occupied by an elementary chain of fixed end-separation vector  $\mathbf{r}_c$ , whether constant or not, is usually much larger than the volume of condensed matter  $v_c = N_c \bar{\omega}_c$  that defines the chain segment ( $N_c$  is the number of skeletal bonds between two consecutive fixed end-points and  $\bar{\omega}_c$  is the average volume per skeletal bond).

However, the full unfolding of elementary chains is known to be considerably hindered by topological constraints resulting, for example, from chain stiffness, monomer-monomer interactions and the presence of crosslinks or junctions. Roughly, it can be considered that the higher the volume occupied by a chain segment, the smaller its configurational entropy reduction and thereby the weaker its elastic behaviour. In other words, the higher the fractal character of a chain segment (swollen gel), the smaller its elastic modulus  $E$  ( $E \propto Q^{-2.25}$  for a gel swelling ratio equal to  $Q$ )<sup>5</sup>. This qualitative assertion stresses the need to evaluate the extent of the chain fractal character in a polymer system, even though it consists of unlabelled macromolecules swollen by one another. Hence, the difficulty is to define an experimental parameter that is connected to individual fractal properties of chains, in a straightforward way.

It has long been observed that strongly entangled chains in a melt or in covalent gels exhibit a residual energy  $\hbar\Delta_r$ , of tensorial spin-spin interactions<sup>6-8</sup>; the order of magnitude of  $\Delta_r/2\pi$  is usually  $10^2$  Hz, for protons attached to polymer chains. The residual energy  $\hbar\Delta_r$ , reflects non-isotropic diffusional rotations of monomeric units; deviations from isotropic motions originate from slight stretchings of chain segments. More precisely,  $\Delta_r$  is induced by a reduction of configurational entropy of chain segments; the smaller the statistical volume occupied by a chain segment, the higher the amplitude of  $\Delta_r$ . In other words,  $1/\Delta_r$  may serve the function of a parameter used to estimate the average individual fractal character of chain segments in a molten polymer system. Whatever the complex nature of the residual energy of dipole-dipole interactions and its exact strength, it has already been shown that it is decreased when the entanglement concentration is lowered by progressively adding a good solvent to long polymer chains<sup>9</sup>.

This work deals with investigations of specific qualitative and quantitative properties of the transverse magnetization of protons, attached to entangled and to crosslinked polymer chains. This experimental approach mainly relies upon the formation of spin echoes originating from the residual energy of spin-spin interactions. The origin of these is similar to that of solid echoes<sup>10</sup>.

More precisely, the purpose of this work is to propose experimental procedures that accurately disclose the existence of a residual energy of interactions in the spin-system response. The aim of the analysis is two-fold:

(i) In the case of molten polymers,  $\Delta_r$  has been shown to serve the function of a reference frequency to characterize the kinetics of chain disentanglement. Accordingly the existence of  $\Delta_r$  must be shown unambiguously.

(ii) In the case of polymeric gels,  $\Delta_r$  must result from an average of residual energies reflecting a distribution of constraints exerted on chain segments. The distribution will be shown to depend upon the state of the gel: dry or swollen. Accordingly, the spin system must be carefully analysed.

### RESIDUAL ENERGY OF SPIN-SPIN INTERACTIONS

The residual energy of dipole-dipole interactions, induced by chain stretching, has already been calculated by considering non-interacting proton pairs located on skeletal bonds of an ideal chain segment subject to a constant force  $\mathbf{f}$ :

$$\varepsilon_e(\mathbf{f}) = \Delta_G [I_{5/2}(u)/I_{1/2}(u)] (3 \cos^2 \theta_f - 1) \quad (1)$$

with  $\Delta_G = 3\gamma_p^2/4d^3$  ( $\Delta_G = 10^5 \text{ rad s}^{-1}$  for  $d = 1.78 \text{ \AA}$ ), where  $\gamma_p$  is the proton gyromagnetic ratio,  $d$  is the distance between nuclei within a proton pair,  $I_{5/2}(u)$  and  $I_{1/2}(u)$  are Bessel functions of the second kind,  $\theta_f$  is the angle that the constant force  $\mathbf{f}$  makes with the steady magnetic field direction,  $u = bf/kT$  and  $b$  is the average length of skeletal bonds<sup>11</sup>. Correspondingly, the state equation of the chain segment, relating the average end-separation vector  $\mathbf{r}_e$  to the applied force  $\mathbf{f}$ , is expressed as<sup>12</sup>:

$$\langle \mathbf{r}_e \rangle_f = bN_e \mathcal{L}(u) \quad (2)$$

where  $\mathcal{L}(u)$  is the well known Langevin function:

$$\mathcal{L}(u) = (\cosh u - u^{-1} \sinh u) / \sinh u$$

Fluctuations of chain dimensions, along the force direction, are described by:

$$\langle (\Delta \mathbf{r}_e)_\parallel^2 \rangle_f = b^2 N_e [1 - \mathcal{L}^2(u) - 2\mathcal{L}(u)/u] \quad (3)$$

with  $\Delta \mathbf{r}_e = \mathbf{r}_e - \langle \mathbf{r}_e \rangle_f$ . Fluctuations of chain dimensions, perpendicular to the force direction, are described by:

$$\frac{1}{2} \langle (\Delta \mathbf{r}_e)_\perp^2 \rangle_f = b^2 N_e \mathcal{L}(u)/u \quad (4)$$

The residual energy  $\varepsilon_e(\mathbf{f})$  is represented as a function of the end-separation vector  $\langle \mathbf{r}_e \rangle_f$  in Figure 1. For slightly stretched chain segments ( $\langle \mathbf{r}_e \rangle_f / bN_e \approx 0.1$ ) the residual energy is expressed as:

$$\varepsilon_e(\langle \mathbf{r}_e \rangle) \approx \Delta_G (3 \cos^2 \theta_e - 1) 3 \langle \mathbf{r}_e \rangle_f^2 / 5b^2 N_e^2 \quad (5)$$

where  $|\varepsilon_e| \approx 6 \times 10^2 \text{ rad s}^{-1}$  for  $\Delta_G = 10^5 \text{ rad s}^{-1}$  in a glass. The residual energy  $\Delta_r$ , measured in a given sample, results from an isotropic average over all end-separation vectors  $\langle \mathbf{r}_e \rangle$ . Correspondingly:

$$\langle (\Delta \mathbf{r}_e)_\parallel^2 \rangle_f \approx \frac{1}{3} b^2 N_e (1 - u^2/5)$$

and

$$\frac{1}{2} \langle (\Delta \mathbf{r}_e)_\perp^2 \rangle_f \approx \frac{1}{3} b^2 N_e (1 - u^2/15)$$

So the statistical volume due to chain fluctuations is about  $N_e^{3/2} b^3$ .

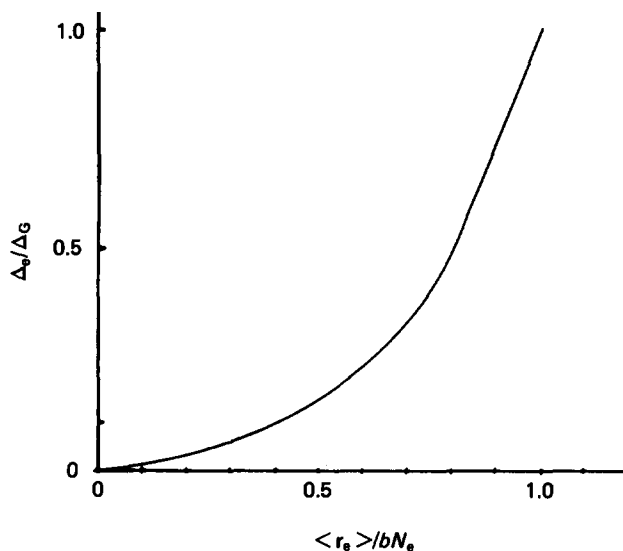


Figure 1 The residual energy  $\Delta_e/\Delta_G = |\varepsilon_e|/\Delta_G$  as a function of the average end-separation vector  $\langle \mathbf{r}_e \rangle / bN_e$  ( $\theta_e = \pi/2$ )

For strong chain stretching ( $\langle \mathbf{r}_e \rangle_f / bN_e \lesssim 1$ ) the residual energy is expressed as:

$$\varepsilon_e(\mathbf{f}) \approx \Delta_G (3 \cos^2 \theta_f - 1) (1 - 3kT/bf)$$

almost equal to its maximum value  $\Delta_G$ . Correspondingly, the volume due to chain fluctuations is negligibly small; the chain segment has lost its fractal character:

$$\langle (\Delta \mathbf{r}_e)_\parallel^2 \rangle_f \approx b^2 N_e (kT/bf)^2$$

and

$$\langle (\Delta \mathbf{r}_e)_\perp^2 \rangle_f \approx 2b^2 N_e (kT/bf)$$

The residual energy  $\varepsilon_e(\mathbf{f})$  is represented as a function of the normalized volume  $V$  given by

$$V = (3/\sqrt{3}) [\langle (\Delta \mathbf{r}_e)_\parallel^2 \rangle_f]^{1/2} \langle (\Delta \mathbf{r}_e)_\perp^2 \rangle_f / 2b^3 N_e^{3/2}$$

in Figure 2. The connection of the residual energy with transverse fluctuations of a chain segment is easily seen from the relationship derived from formulae (1) and (4):

$$\frac{|\varepsilon_e|}{\Delta_G} + \frac{3 \langle (\Delta \mathbf{r}_e)_\perp^2 \rangle_f}{2b^2 N_e} = 1$$

for  $\theta_f = \pi/2$ .

The above results apply qualitatively to real chains too; the skeletal stiffness probably increases deviations of diffusional rotations of monomeric units from isotropic motions. Interactions of monomeric units with one another also partly govern rotational diffusions<sup>13</sup>. Furthermore, nuclear spins cannot be considered as forming separate proton pairs; all spins located either within a given chain segment or on different segments interact with one another. Therefore, all spin-spin interactions must be taken into account in the spin Hamiltonian of the polymer systems. A residual energy of dipole-dipole interactions may originate from spins located on different chain segments because of orientational interactions of monomeric units<sup>14,15</sup>.

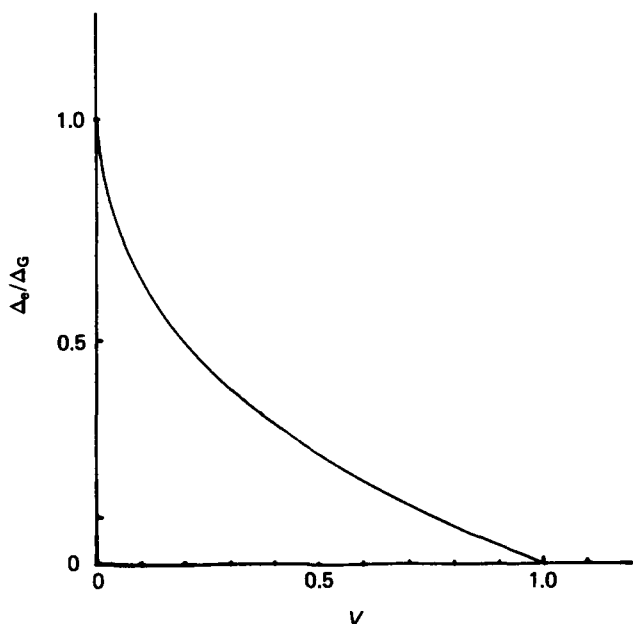


Figure 2 The residual energy  $\Delta_e/\Delta_G = |\epsilon_e|/\Delta_G$  as a function of the average volume  $V$  due to chain fluctuations,  $V = (3\sqrt{3})\langle(\Delta\epsilon_e)_\perp^2\rangle r[\langle(\Delta r_e)_\parallel^2\rangle]^{1/2}/2b^3N_e^{3/2}$

### TRANSVERSE MAGNETIZATION DYNAMICS

It is worth emphasizing that pseudo-solid n.m.r. properties observed in molten polymer systems will be described from the adiabatic part of the residual energy of dipole-dipole interactions of spins; it is the part that commutes with the Zeeman energy of the spin system and it induces slight shifts of Zeeman energy levels. The fluctuating non-adiabatic part of the interaction energy of nuclear spins and its reduced fluctuating adiabatic part are responsible for the spin-spin relaxation process in the usual way. They contribute to the relaxation of the transverse magnetic component in addition to the residual energy effect<sup>16</sup>.

The density matrix describing the spin-system response in the frame rotating at the Larmor frequency of protons can be written as:

$$\rho^*(t) = e^{i\mathcal{H}_e t} \rho_e^*(t) e^{-i\mathcal{H}_e t} \quad (6)$$

where  $\mathcal{H}_e$  is the residual energy of spin-spin interactions and  $\rho^*(t)$  is the density matrix part describing quantum phase coherence properties of spins only. It is represented by non-diagonal elements in the basis defined from eigenfunctions of the Zeeman energy. The dynamics of the operator  $\rho_e^*(t)$  originate from the fluctuating part  $[\mathcal{H}_D(t) - \mathcal{H}_e]$  of spin-spin interactions  $\mathcal{H}_D(t)$ . It will be experimentally shown in a later section that  $\rho_e^*(t)$  is a very slowly varying function of time. Consequently, it is assumed that all elements of  $\rho_e^*(t)$  can be described from a single decreasing function of time:  $\phi_e(t)$ . The transverse magnetization is written as:

$$M_x^*(t) = M_x^c(t) \phi_e(t) \quad (7)$$

with

$$M_x^c(t) = \langle e^{i\mathcal{H}_e t} \mathcal{M}_x e^{-i\mathcal{H}_e t} \mathcal{M}_x \rangle \quad (8)$$

Dynamic properties of  $M_x^c(t)$  are induced by the adiabatic residual energy  $\mathcal{H}_e$  of spin-spin interactions.

Interchain segment magnetic interactions  $\mathcal{H}_e^i$  and intrachain segment ones  $\mathcal{H}_e^c$  are included in  $\mathcal{H}_e$ .  $\mathcal{M}_x$  is the total  $x$  component of nuclear magnetic dipoles and  $\langle A \rangle$  means a trace of operator  $A$  divided by  $\text{Tr}(\mathcal{M}^2 x)$ . The  $\phi_e(t)$  function accounts for effects of the fluctuating parts of the dipole-dipole energy of spin interactions. The two contributions  $M_x^c(t)$  and  $\phi_e(t)$  are decoupled from each other within a good approximation;  $\phi_e(t)$  will be set equal to 1 throughout the present description. Echoes resulting from the presence of a residual energy have been called pseudo-solid because they originate from spin-spin interactions that are not constant but fluctuate permanently.

### EXPERIMENTAL PROCEDURE

To realize the spin-echo sequences described below, a pulsed n.m.r. spectrometer capable of delivering trains of pulses of different carrier phases is a necessity. The experiments depicted in this paper were carried out on a CXP-Bruker spectrometer operating at 60 MHz. The  $(\frac{1}{2}\pi)$  and  $(\pi)$  pulses applied at resonance along the  $x$ ,  $-x$ ,  $y$  and  $-y$  axes have to be adjusted beforehand with great accuracy. As the r.f. field must be as homogeneous as possible over the sample volume, it is advisable to work on small samples.

Compared with dipolar solids where the nuclear magnetization decays in a very short time ( $\approx 10^{-5}$  s), polymers have relatively long relaxation decays ( $\approx 10^{-2}$  s). This enables us to carry out multiple pulse experiments without great difficulties. A dwell time of 4  $\mu$ s is quite sufficient to get well resolved spectra, the minimal pulse spacing being about 50  $\mu$ s.

The sequences are intended for inhomogeneous systems where the dispersal of precession rates of the nuclei precludes standard solid echo measurements<sup>10</sup>. The typical phaseshifted  $(\frac{1}{2}\pi)$  pulses are applied on the stroboscopically focused magnetization by means of modified Hahn or Carr-Purcell techniques.

#### Pseudo-solid echo measurement

The basic experiment to observe a pseudo-solid echo in an inhomogeneous sample is the following four-pulse sequence:

$$(\frac{1}{2}\pi/y) - \frac{1}{2}\tau - (\pi/y) - \frac{1}{2}\tau - (\frac{1}{2}\pi/-x) - \frac{1}{2}\tau_1 - (\pi/y)$$

The amplitude of the transverse magnetization along the  $x$ -axis measured at time  $\tau + \tau_1$  gives the corresponding value of the pseudo-solid echo envelope.

In order to observe the whole pseudo-solid echo envelope by a single sequence, we may graft a Carr-Purcell pulse train on the preceding sequence. The whole experiment is then featured by the following chain<sup>17</sup>:

$$(\frac{1}{2}\pi/y) - \frac{1}{2}\tau - (\pi/y) - \frac{1}{2}\tau - (\frac{1}{2}\pi/-x) - [\frac{1}{2}\tau_1 - (\pi/y) - \frac{1}{2}\tau_1 - \frac{1}{2}\tau_1 - (\pi/-y) - \frac{1}{2}\tau_1 - \frac{1}{2}\tau_1 - (\pi/-y) - \frac{1}{2}\tau_1 - \frac{1}{2}\tau_1 - (\pi/y) - \frac{1}{2}\tau_1 - \dots]_N$$

#### Multiple pseudo-solid echo sequence

In order to average out the dipolar interactions completely, we produce a sustained pseudo-solid echo chain by applying the following multiple-pulse sequence:

$$(\frac{1}{2}\pi/y) - \frac{1}{2}\tau - (\pi/y) - \frac{1}{2}\tau - [(\frac{1}{2}\pi/-x) - \frac{1}{2}\tau_1 - (\pi/y) - \frac{1}{2}\tau_1 - (\frac{1}{2}\pi/x) - \frac{1}{2}\tau_1 - (\pi/y) - \frac{1}{2}\tau_1 - \dots]_N$$

This sequence proves equivalent to:

$$\begin{aligned} & (\frac{1}{2}\pi/y) - \frac{1}{2}\tau - (\pi/y) - \frac{1}{2}\tau - [(\frac{1}{2}\pi/x) - \frac{1}{2}\tau_1 - (\pi/y) - \frac{1}{2}\tau_1 \\ & - (\frac{1}{2}\pi/x) - \frac{1}{2}\tau_1 - (\pi/y) - \frac{1}{2}\tau_1 - (\frac{1}{2}\pi/x) - \frac{1}{2}\tau_1 - (\pi/-y) \\ & - \frac{1}{2}\tau_1 - (\frac{1}{2}\pi/x) - \frac{1}{2}\tau_1 - (\pi/-y) - \frac{1}{2}\tau_1 - ]_N \end{aligned}$$

Except for initial oscillations, which depict the gradual elimination of the dipolar spin Hamiltonian, we observe a considerably prolonged transverse nuclear magnetization decay<sup>18</sup>.

**Samples**

We illustrate the properties of the pseudo-solid echo sequences from the following samples:

*Sample A.* Crosslinked polybutadiene chains (8% 1,2; 50% *trans*; 42% *cis*) of molecular weight  $M_w = 428\,000$ .

*Sample B.* Crosslinked polybutadiene chains (the same as A) swollen at equilibrium with deuterated cyclohexane.

*Sample C.* Entangled polybutadiene chains (19.6%, 1,2; 46.3% *trans*; 34.1% *cis*) of molecular weight  $M_w = 360\,000$ .

*Sample D.* Entangled polybutadiene chains (8% 1,2; 52% *trans*; 40% *cis*) of molecular weight  $M_w = 50\,000$ .

*Sample E.* Entangled polyethylene chains ( $d = 0.953$ ) of molecular weight  $M_w = 216\,000$ .

*Sample F.* Crosslinked polyethylene chains ( $d = 0.953$ ) of molecular weight  $M_w = 216\,000$ .

*Sample G.* Short polyethylene chains of molecular weight  $M_w = 6300$ .

**CROSSLINKED AND/OR HIGHLY ENTANGLED CHAINS**

Considering crosslinked and/or highly entangled chains, the pseudo-solid echoes obtained according to the experimental procedure described in the previous section exhibit several characteristic properties, which are now described. The irreversible dynamics of the magnetization starts at  $t = 0$ . At  $t = 0_+$  the magnetization  $M_0$  is brought into coincidence with the  $x$ -axis direction (positive values of  $x$ ) in the rotating frame. Then, at  $t = \tau_+$ , a radiofrequency pulse is applied to the spin system; it is assumed to induce a  $\frac{1}{2}\pi$  rotation of nuclear spins around the  $x$ -axis. The equivalent matrix applied to spin operators will be called  $R$ .

The adiabatic part  $\mathcal{H}_e$  of the residual dipole-dipole interaction obeys several elementary properties.

(a) Let  $q_n$  denote the product  $R^n$ . Then:

$$\mathcal{H}_e = q_n \mathcal{H}_e q_n^{-1}$$

if  $n = 2j$  ( $j$  is an integer), and:

$$\mathcal{H}_e^* = q_n \mathcal{H}_e q_n^{-1} = R \mathcal{H}_e R^{-1}$$

if  $n = 2j + 1$ ;  $q_n^{-1} = (R^{-1})^n$ .

(b)  $\mathcal{H}_e$  and  $\mathcal{H}_e^*$  do not commute with each other:

$$[\mathcal{H}_e^*, \mathcal{H}_e] \neq 0$$

(c) Considering the total transverse magnetization operator  $\mathcal{M}_x$ , in the rotating frame, then:

$$[\mathcal{H}_e^*, \mathcal{M}_x] = -[\mathcal{H}_e, \mathcal{M}_x]$$

The above three properties are shown in Appendix A.

At  $t = 0_+$ , the density matrix operator  $\rho(0_+)$  is set equal to  $\rho(0_+) = \mathcal{M}_x$ . A  $(\frac{1}{2}\pi/x)$  pulse is applied to the spin system at  $t = \tau$ . Then, at  $t = \tau_-$ :

$$\rho(\tau_-) = e^{i\mathcal{H}_e \tau} \mathcal{M}_x e^{-i\mathcal{H}_e \tau}$$

and at  $t = \tau_+$ :

$$\rho(\tau_+) = T_1(\tau) \mathcal{M}_x T_1^{-1}(\tau)$$

with

$$T_n(\tau) = e^{i(a_n H_e q_n^{-1})\tau} \quad n = 0, 1, 2, \dots$$

A second  $(\frac{1}{2}\pi/x)$  pulse is applied at  $t = 2\tau$ . Then, at  $t = 2\tau_-$ :

$$\rho(2\tau_-) = T_0(\tau) T_1(\tau) \mathcal{M}_x T_1^{-1}(\tau) T_0^{-1}(\tau)$$

and at  $t = 2\tau_+$ :

$$\rho(2\tau_+) = T_1(\tau) T_2(\tau) \mathcal{M}_x T_2^{-1}(\tau) T_1^{-1}(\tau)$$

The echo function is expressed as:

$$\tilde{M}_x^e(t > \tau) = \langle T_0^{-1}(t - \tau) \mathcal{M}_x T_0(t - \tau) T_1(\tau) \mathcal{M}_x T_1^{-1}(\tau) \rangle \quad (9)$$

where  $T_0(\tau) = e^{i\mathcal{H}_e \tau}$

*Symmetry property at  $t = \tau_+$*

The slope of the echo function at  $t = \tau_+$  is derived from:

$$\left. \frac{d\tilde{M}_x^e(t > \tau)}{dt} \right|_{t=\tau_+} = \langle -i[\mathcal{H}_e, \mathcal{M}_x] T_1(\tau) \mathcal{M}_x T_1^{-1}(\tau) \rangle$$

or, by including the unity transformation  $RR^{-1}$  in the trace:

$$\left. \frac{d\tilde{M}_x^e(t > \tau)}{dt} \right|_{t=\tau_+} = -\langle i[\mathcal{H}_e^*, \mathcal{M}_x] T_2(\tau) \mathcal{M}_x T_2^{-1}(\tau) \rangle$$

and finally:

$$\left. \frac{d\tilde{M}_x^e(t > \tau)}{dt} \right|_{t=\tau_+} = -\left. \frac{dM_x(t)}{dt} \right|_{t=\tau_-} \quad (10)$$

The slope of the echo function at  $t = \tau_+$  must be exactly the opposite of the slope of the relaxation function at  $t = \tau_-$ . This typical property is illustrated in *Figure 3*. Pseudo-solid spin echoes observed in a dry polybutadiene network (sample A) and in a swollen polybutadiene network (sample B) are shown in *Figures 3a* and *3b*; they were formed at room temperature. Pseudo-solid echoes observed in crosslinked polyethylene chains (sample F) are reported in *Figure 3c*; they were formed at 418 K.

*Echo property as a function of  $\tau$*

Given a fixed value  $t$ , the expression (8) is now considered as a function of  $\tau < t$ . Characteristic values of this function are  $M_x^e(t)$  for  $\tau = t$  and  $\tau = 0$ . It is symmetrical with respect to  $\tau = t/2$ . Let  $u$  denote the difference  $t/2 - \tau$ . Then:

$$\tilde{M}_x^e(t; u) = \langle T_0^{-1}(t/2 + u) \mathcal{M}_x T_0(t/2 + u) T_1(t/2 - u) \mathcal{M}_x T_1^{-1}(t/2 - u) \rangle$$

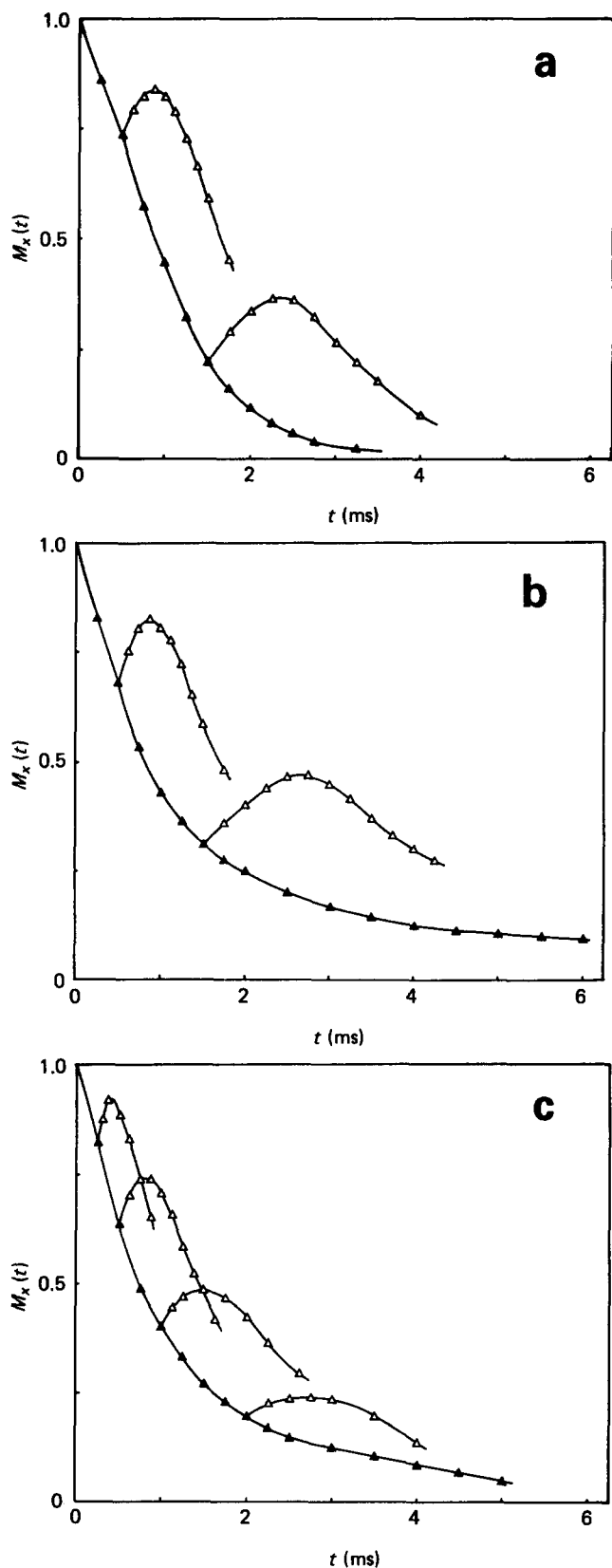


Figure 3 Transverse magnetic relaxation functions (▲) and pseudo-solid spin echoes (△) for several times  $\tau$ . Experimental curves were observed for: (a) sample A at  $T=300$  K; (b) sample B at  $T=300$  K; (c) sample C at  $T=418$  K

Replacing  $u$  with  $-u$  and including  $RR^{-1}$  in the trace:

$$\tilde{M}_x^e(t; -u) = \langle T_2(t/2+u) \mathcal{M} x T_2^{-1}(t/2+u) T_1^{-1}(t/2-u) \mathcal{M} x T_1(t/2-u) \rangle$$

$\tilde{M}_x^e(t; -u)$  is easily shown to be equal to  $\tilde{M}_x^e(t; u)$ , which is

a real function; the maximum occurs for  $u=0$ . Three typical  $\tilde{M}_x^e(t; u)$  functions, drawn for fixed  $t$  values, are reported in Figure 4. They were built from pseudo-solid spin echoes observed in dry and swollen crosslinked polybutadiene chains (samples A and B).

Intersection of pseudo-solid echoes

Starting from a time interval  $\tau$ , echo functions  $\tilde{M}_x^e(t > \tau - \eta)$  and  $\tilde{M}_x^e(t > \tau + \eta)$  are considered. It is now shown that their intercept corresponds to  $t = 2\tau$ . On the one hand:

$$\tilde{M}_x^e(2\tau; \tau - \eta) = \langle T_0^{-1}(\tau + \eta) \mathcal{M} x T_0(\tau + \eta) T_1(\tau - \eta) \mathcal{M} x T_1^{-1}(\tau - \eta) \rangle$$

and on the other:

$$\tilde{M}_x^e(2\tau; \tau + \eta) = \langle T_0^{-1}(\tau - \eta) \mathcal{M} x T_0(\tau - \eta) T_1(\tau + \eta) \mathcal{M} x T_1^{-1}(\tau + \eta) \rangle$$

Or,

$$\tilde{M}_x^e(2\tau; \tau + \eta) = \langle T_2(\tau + \eta) \mathcal{M} x T_2^{-1}(\tau + \eta) T_1^{-1}(\tau - \eta) \mathcal{M} x T_1^{-1}(\tau - \eta) \rangle$$

Therefore,  $\tilde{M}_x^e(2\tau; \tau + \eta)$  is equal to  $\tilde{M}_x^e(2\tau; \tau - \eta)$ , which is a real function. Several intersections of pseudo-solid echoes are shown in Figure 5. Echoes were formed from dry and swollen polybutadiene networks (samples A and B).

Approximate echo function expression

The exact calculation of the echo function is a difficult problem, which cannot be overcome, except for very specific simple spin systems. However,  $\tilde{M}_x^e(t > \tau)$  may be expressed as:

$$\tilde{M}_x^e(t > \tau) = \langle T_1(t - \tau) T_0^{-1}(t - \tau) T_0(t) \mathcal{M} x T_0^{-1}(t) T_0(t - \tau) T_1^{-1}(t - \tau) \mathcal{M} x \rangle$$

This expression is now written as a series expansion of the time variable  $t - \tau$  while the coefficients of this series

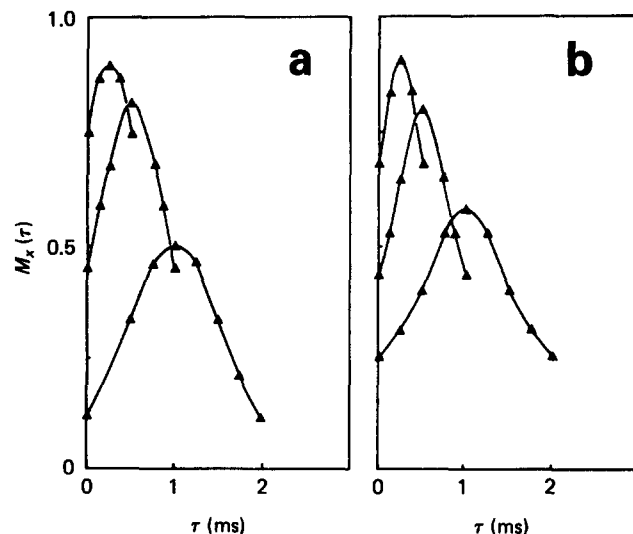


Figure 4 Spin-echo functions  $\tilde{M}_x^e(t; \tau)$  observed at a fixed time  $t$  as a function of the spin-echo origin  $\tau < t$ . Three fixed  $t$  values were chosen ( $t=0.5, 1$  and  $2$  ms). (a) Sample A at  $300$  K; (b) sample B at  $300$  K

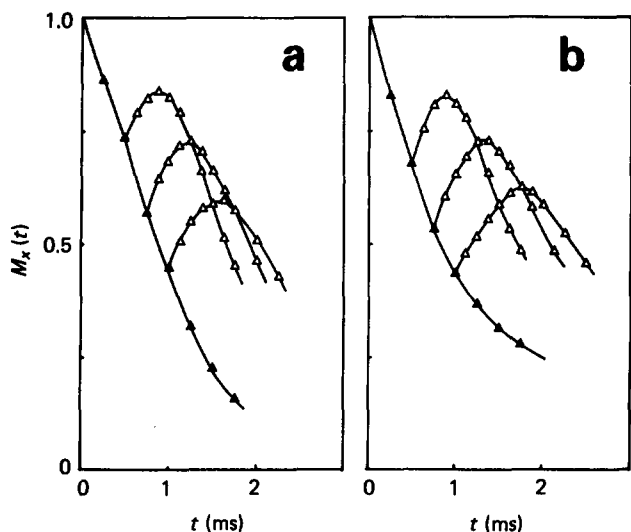


Figure 5 Spin echoes for  $(\frac{1}{2}\pi/x)$  pulses applied at times  $\tau + \eta$  and  $\tau - \eta$  interact at time  $2\tau$ . This is illustrated by spin echoes measured in the following samples: (a) sample A at  $T = 300$  K; (b) sample B at  $T = 300$  K

are defined from derivatives of  $T_0(t) \cdot M_x T_0^{-1}(t)$ :

$$\tilde{M}_x^c(t > \tau) = M_x^c(t) - 2(t - \tau)\dot{M}_x^c(t) - (t - \tau)^2 [2M_2^c(t) + A^c(t)] + \dots \quad (11)$$

$\dot{M}_x^c(t)$  is the first time derivative of the magnetization. Also:

$$M_2^c(t) = \langle [\mathcal{H}_e, [\mathcal{H}_e, M_x(t)]] \cdot M_x \rangle$$

and:

$$A^c(t) = \frac{1}{2} \langle [\mathcal{H}_e^*, [\mathcal{H}_e^* + \mathcal{H}_e, M_x(t)]] \cdot M_x \rangle$$

$M_2^c(t)$  and  $A^c(t)$  obey the relationships:

$$M_2^c(0) = M_2^c \quad \text{and} \quad A^c(0) = 0$$

where  $M_2^c$  is the second moment of the resonance line resulting from the Fourier transform of  $M_x(t)$ . The echo function  $\tilde{M}_x^c(t > \tau)$  may be written more generally as:

$$\tilde{M}_x^c(t > \tau) = M_x^c(t) + (t - \tau)f(t - \tau; t) \quad (12)$$

The function  $f(t - \tau; t)$  goes to  $-2\dot{M}_x^c(t)$  when  $t$  goes to  $\tau$ .

Functions  $[\tilde{M}_x^c(t) - M_x^c(t)] / (t - \tau)$  for different  $\tau$  values are drawn from spin echoes observed in samples A and B in Figure 6. The function  $f(t - \tau)$  proves to be a linear function of  $t - \tau$  for small  $t - \tau$  values. Its slope is an estimate of  $A^c(\tau)$ .

Although the following parameter  $\xi(\tau)$  cannot be given a quantitative interpretation, it may lead to a useful qualitative characterization of the transverse relaxation function. The parameter  $\xi(\tau)$  is defined by the ratio  $\xi(\tau) = 2\tau/T$  and  $T$  by  $\tilde{M}_x^c(2\tau, \tau) = M_x^c(T)$ .

High  $\xi(\tau)$  values represent strong dipolar interactions whereas  $\xi$  goes to 1 for vanishing interactions. Variations of the parameter  $\xi(\tau)$  are reported in Figure 7 as a function of  $\tau$  for samples A and B. The experimental curves clearly illustrate both the increase of  $\Delta_r$  due to the stretching effect of elementary chains in a swollen network structure and the change of the distribution function of the residual energy along segments connecting junctions.

RAPIDLY FLUCTUATING ENTANGLEMENTS

Spin-echo properties described in the foregoing section are now contrasted with those observed in molten polymer systems where entanglements rapidly fluctuate with respect to the timescale defined by  $(\Delta_r/2\pi)^{-1}$ . The relaxation time of disentanglement,  $T_R$ , is known to be strongly dependent upon the chain molecular weight  $M$ :

$$T_R \propto M^\alpha \quad \text{with } \alpha \approx 3$$

This dependence has been predicted from the reptational motion proposed by De Gennes<sup>5</sup>. The relaxation rate  $T_R^{-1}$  may be rendered shorter than or equal to the residual energy  $\Delta_r$  by decreasing  $M$  in an appropriate way. Spin echoes formed from short uncrosslinked polybutadiene chains ( $M_w = 0.5 \times 10^5$ , sample D) are reported in Figure 8a. They do not obey any characteristic behaviour: neither symmetry properties of slopes at  $t = \tau_+$  or of echo functions of  $\tau$  (Figure 8b), nor intersections of echoes exhibit specific aspects mentioned in the previous section. Values of  $\xi(\tau)$  are reported in Figure 7. Although entanglements exist, they dissociate within a timescale short enough compared with  $(\Delta_r/2\pi)^{-1} \approx 1.5 \times 10^3$  s for the observed sample. Considering n.m.r. properties the residual energy now appears at a fluctuating time function.

Echoes were also formed from uncrosslinked polyethylene ( $M_w \approx 2.15 \times 10^5$ , sample E). They were not found to exhibit any characteristic behaviour associated with a transverse magnetization governed by a static residual energy (Figure 9a). It must be concluded that entanglements fluctuate within a timescale shorter than  $(\Delta_r/2\pi)^{-1} \approx 1.25 \times 10^{-3}$  s, although polymer chains have a high molecular weight. The corresponding  $\xi(\tau)$  values are reported in Figure 9b and are found to be much smaller than those measured from crosslinked polyethylene.

It may be worth emphasizing that average molecular weights of chain segments joining two consecutive entanglements are currently considered as equal to about 2500 and 1250 for polybutadiene and polyethylene, respectively<sup>1</sup>. Correspondingly, the number of sub-molecules per chain is equal to  $2.15 \times 10^5 / 1250$  in the

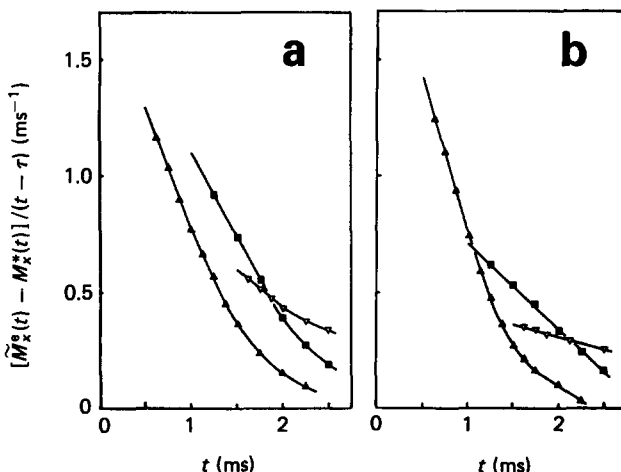
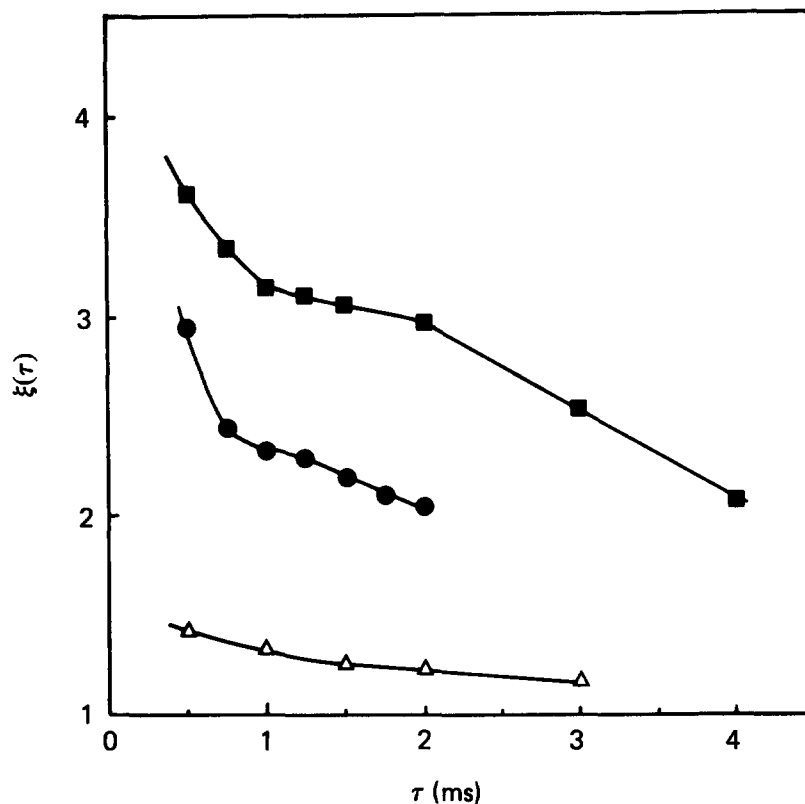


Figure 6 Spin echoes  $\tilde{M}_x^c(t)$  at various times  $\tau$  at time  $t > \tau$  and compared with the relaxation function  $M_x^c(t)$  through the function  $[\tilde{M}_x^c(t) - M_x^c(t)] / (t - \tau)$ . Three fixed  $\tau$  values were chosen: ( $\blacktriangle$ )  $\tau = 0.5$  ms; ( $\blacksquare$ )  $\tau = 1$  ms; ( $\nabla$ )  $\tau = 1.5$  ms. (a) Sample A at  $T = 300$  K; (b) sample B at  $T = 300$  K

polyethylene sample, while it is equal to  $3.6 \times 10^5/2500$  per chain in the high-molecular-weight polybutadiene sample (sample C). Spin echoes drawn in sample C, however, obey the characteristic symmetry properties described in the previous section (Figure 9c).

The present analysis clearly shows that the chain migration process is faster in polyethylene although the

number of submolecules per chain is higher than in the polybutadiene sample. This result must be related to a friction constant higher in the latter polymer system than in the former<sup>19</sup>. Furthermore, in no case could the relaxation rate determined from relaxation functions observed in uncrosslinked polyethylene or in uncrosslinked polybutadiene ( $M \approx 5 \times 10^5$ ) serve the



**Figure 7** Functions  $\xi(\tau)$  for three different polybutadiene samples at  $T = 300$  K: (●) crosslinked chains,  $M_w = 428\,000$ , sample A; (■) crosslinked chains, swollen at equilibrium, sample B; (△) entangled chains,  $M_w = 50\,000$ , sample D

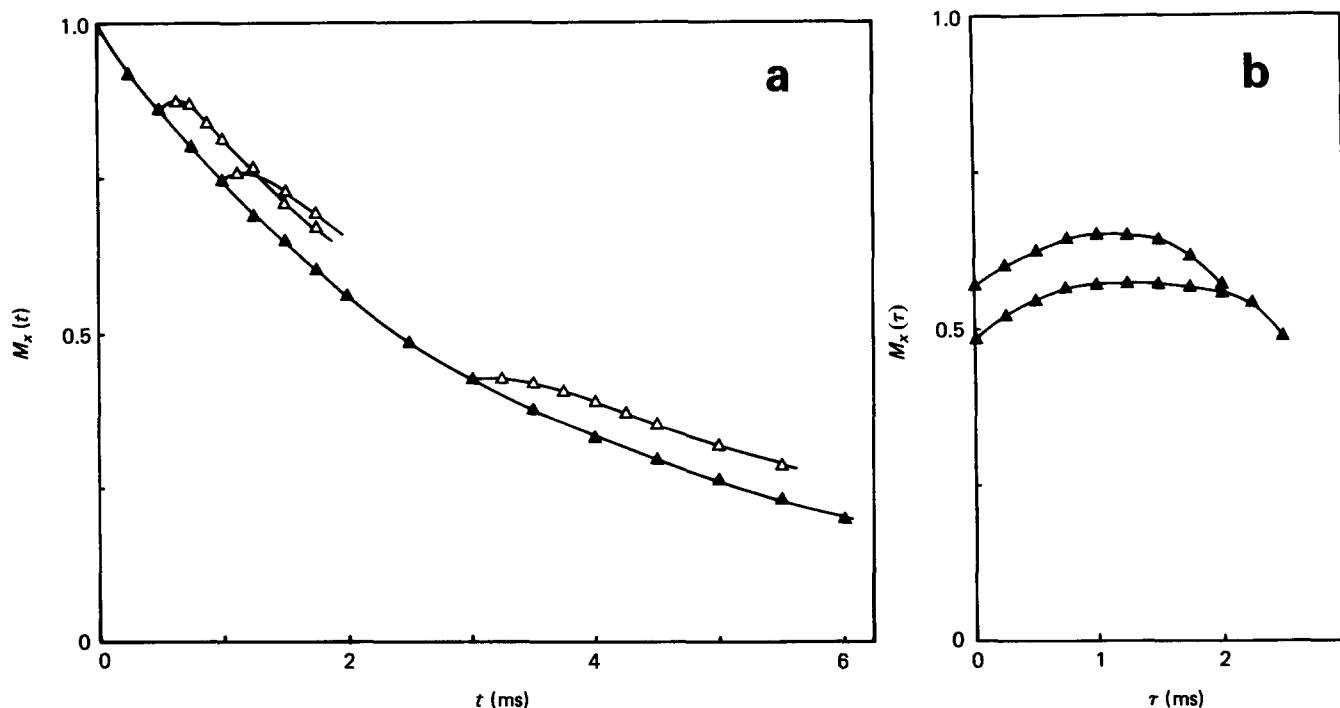


**Figure 8** (a) Transverse magnetic relaxation function (▲) and pseudo-solid spin echoes (△) observed for entangled polybutadiene chains (sample D) at  $T = 300$  K. (b) Spin-echo functions  $M_x^e(t; \tau)$  observed at two fixed  $t$  values ( $t = 2$  and  $2.5$  ms) as a function of the spin-echo origin  $\tau < t$  are non-symmetric about  $t/2$  for sample D ( $T = 300$  K)

function of a reference frequency because it does not represent a pure residual energy of spin interactions.

**HIGH-FREQUENCY ROTATIONAL PROCESSES**

Turning back to formula (7), the purpose of the experimental approach now described was to eliminate the residual energy from the spin-system response to disclose effects of high-frequency rotational diffusion processes of monomeric units. Magic-angle spinning is

known to reduce tensorial interactions of spins to zero. However, strong diamagnetic inhomogeneities occurring in crosslinked materials and loaded polymer systems cannot be eliminated completely, using such an experimental procedure only. This necessitates application of multiple-pulse sequences to the spin system. More precisely, specific pulses that eliminate the residual energy of spin interactions must be combined with pulses that focus the magnetization along a given axis, in the frame rotating at the Larmor frequency. The multiple-

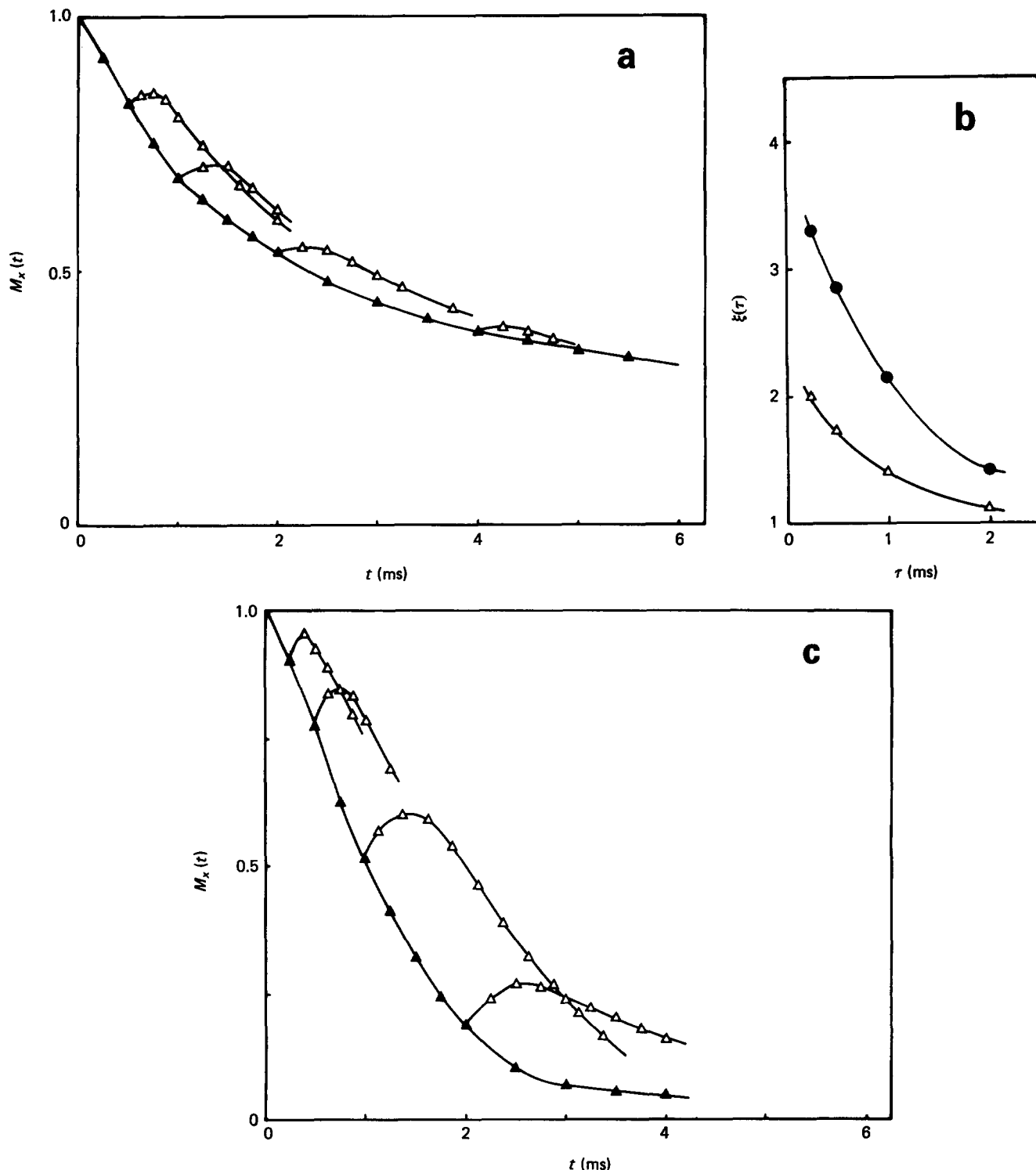


**Figure 9** (a) Polyethylene chains (sample E): transverse magnetic relaxation function ( $\blacktriangle$ ) and pseudo-solid spin echoes ( $\triangle$ ) ( $T=418$  K). (b) Comparison of functions  $\zeta(\tau)$  for entangled polyethylene chains ( $\triangle$ ) (sample E) and crosslinked polyethylene chains ( $\bullet$ ) (sample F) ( $T=418$  K). (c) Polybutadiene chains (sample C): transverse magnetic relaxation functions ( $\blacktriangle$ ) and pseudo-solid spin echoes ( $\triangle$ ) ( $T=300$  K)



pulse sequence described in the earlier section was applied to the polybutadiene samples. The effect of such a pulse sequence upon the spin-system response is analysed in Appendix B, in the case where the time interval  $\tau$  between successive pulses is short compared with  $(\Delta_r/2\pi)^{-1}$ . The residual interaction of spins is considered as a time function; it has alternate expressions  $\mathcal{H}_e$  and  $\mathcal{H}_e^*$ , over two successive time intervals  $\tau$ . A motional averaging process is thus induced in spin space. It is not the purpose of the present work to give a detailed discussion of such a known effect. The relaxation function can be expressed within a conventional framework of calculation<sup>16</sup>. It is a pure exponential time function for short  $\tau$  values:

$$M_x^r(t) = e^{-M_2^r t/2}$$

By choosing  $\tau$  in an appropriate way, the rate constant  $M_2^r\tau/2$  may be smaller than the rate constant characterizing the  $\phi_e(t)$  function in formula (7). The elimination effect of the residual energy upon the irreversible behaviour of the magnetization is illustrated in Figure 9. Three different polybutadiene samples were observed.

(i) Results concerning a crosslinked sample, characterized by a molecular weight  $M_w \approx 4.28 \times 10^5$  (sample A), are reported in Figure 10a; experimental points represent a slowly decreasing relaxation function  $\phi_e^a(t)$ .

(ii) Then, the remaining function  $\phi_e^b(t)$  was also drawn from an uncrosslinked sample characterized by a low molecular weight  $M_w \approx 0.5 \times 10^5$  (sample D, Figure 10b).

(iii) Finally, the function  $\phi_e^c(t)$ , concerning a crosslinked sample ( $M_w \approx 4.28 \times 10^5$ , sample B) swollen by a good solvent, was reported in Figure 10c.

It is worth noting that the observed  $\phi_e(t)$  does not depend upon the time-interval length  $\tau_1$ , provided it is shorter than  $\Delta_r/2$ .

Two features in accordance with general properties of polymer systems are clearly seen from the three parts of Figure 10. Remaining functions  $\phi_e^a(t)$  and  $\phi_e^b(t)$  were found to have the same relaxation rate although they were observed in very different polymer systems. In one of them, formed from short chains, entanglement fluctuations are fast enough to be perceived from n.m.r., as was explained in an earlier section. In the other polymer system, formed from long chains ( $M_w \approx 4.28 \times 10^5$ ), entanglements slowly fluctuate or are even frozen by crosslink points. Thus, similar properties of functions  $\phi_e^a(t)$  and  $\phi_e^b(t)$  clearly indicate that they are not sensitive to long-range fluctuations in polymer systems. High relaxational frequency motions (also called local fluctuations) are independent of long-range properties; these are screened within small space domains. Such a result is in accordance with the independence of high-frequency viscoelastic properties observed with respect to the chain molecular weight of a polymer system.

Furthermore, the other feature concerns the addition of solvent to the crosslinked polybutadiene system. Deuterated cyclohexane is a good solvent. The rate constant of the remaining function  $\phi_e^c(t)$  was found to be decreased compared with that of  $\phi_e^a(t)$  when the gel is swollen at equilibrium with the liquid solvent. Thus, local fluctuations are given more freedom by adding a solvent to a crosslinked system, as is expected.

Therefore, the elimination of the residual energy of spin-spin interactions clearly shows that the transverse

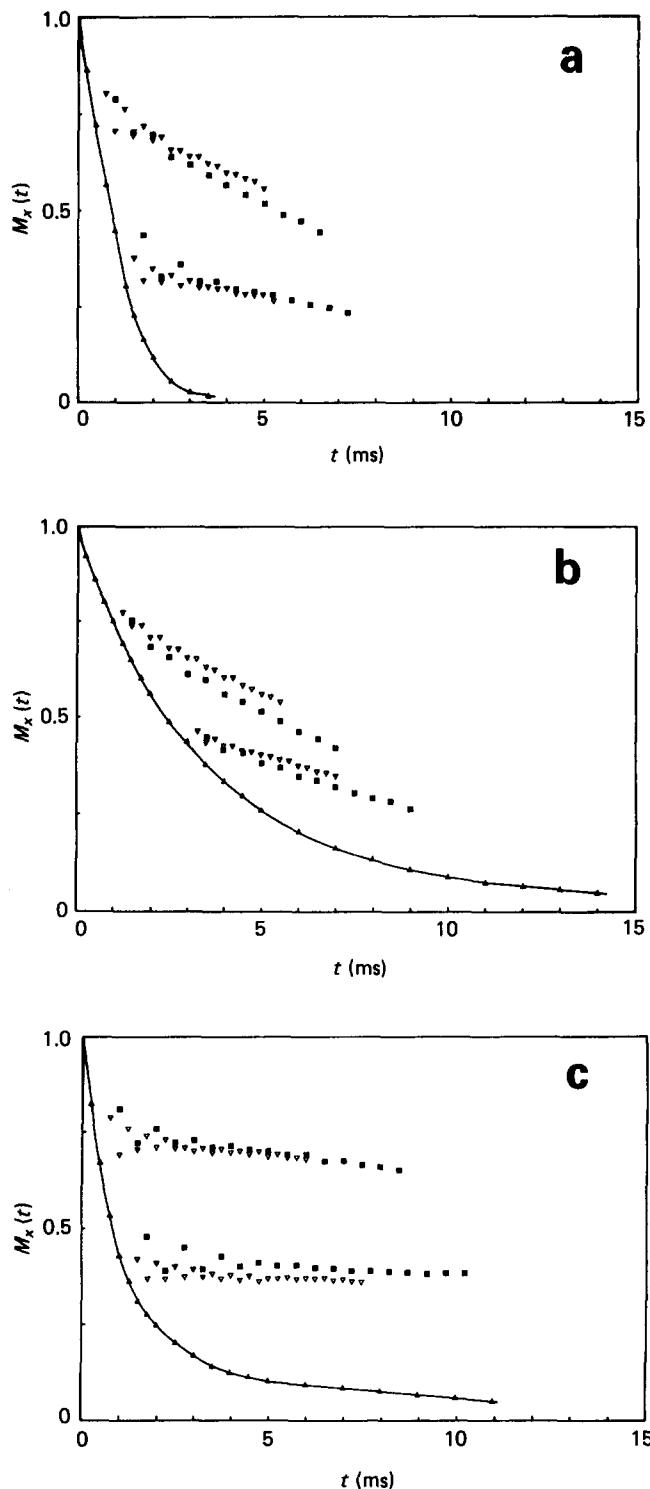


Figure 10 Transverse magnetic relaxation functions ( $\blacktriangle$ ) and effect of the multiple-pulse sequence described in the fourth section observed for different  $\tau_1$  values: ( $\nabla$ )  $\tau_1 = 0.25$  ms; ( $\blacksquare$ )  $\tau_1 = 0.5$  ms. (a) Sample A at  $T = 300$  K,  $\tau$  values are 0.5 and 1.25 ms; (b) sample D at  $T = 300$  K,  $\tau$  values are 1 and 3 ms; (c) sample B at  $T = 300$  K,  $\tau$  values are 0.5 and 1.25 ms

magnetization consists of two components: that due to rapidly fluctuating properties gives a negligible contribution to the irreversible behaviour of the magnetization.

Finally, the function  $\phi_e(t)$  was drawn from short polyethylene chains ( $M_w = 6300$ , sample G). No more residual spin interactions are seen in this sample and the function  $\phi_e(t)$  coincides with the transverse nuclear magnetization  $M_x(t)$  (Figure 11).

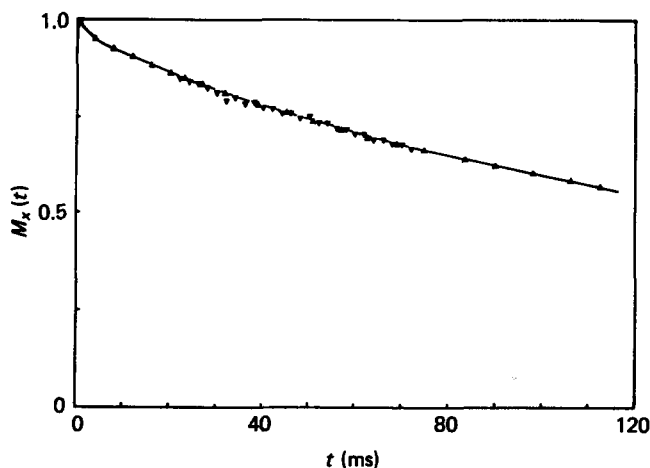


Figure 11 Short polyethylene chains (sample G): the signal produced by a multiple-pulse sequence (∇) is coincident with the transverse magnetic relaxation function (▲):  $\tau = 20$  ms,  $\tau_1 = 2$  ms;  $T = 418$  K

### CONCLUSIONS

N.m.r. can be used to investigate three specific properties of molten polymer systems. The first concerns high-frequency properties associated with diffusional motions of monomeric units and short segments. These properties are molecular-weight-independent and govern high-frequency mechanical responses of polymer systems. They can be investigated from the description of spin-lattice relaxation mechanisms of nuclei attached to chains.

The secondary specific property concerns the low-frequency behaviour of molten polymer systems observed in a semi-local scale. They are associated with a strong molecular-weight dependence. They can be investigated from the transverse magnetic relaxation function, which mainly reflects quantum coherence properties of nuclear spins.

Finally, the third specific property concerns the static scaling behaviour of chain segments: whether they are embedded in a permanent gel or in a temporary network structure determined by entangled long chains. Although the residual energy of tensorial spin-spin interactions may originate from complex physical interactions of monomeric units, it can be used to investigate the fractal character of these chain segments. This applies to swollen gels as well as to unlabelled chain segments swollen by one another. The purpose of the present work was to propose a method of characterization of the transverse magnetization of protons attached to polymer chains. The method must be used to disclose the existence of a residual energy of spin-spin interactions and to determine whether or not its fluctuations are seen from n.m.r. The sensitivity of n.m.r. to these fluctuations implies that disentanglement processes can be observed from the transverse magnetic relaxation function. When fluctuations do not govern the spin-system response, the residual energy appears as a static parameter, which can be used to characterize internal fractal chain structures in complex polymer systems comprising crystallites, covalent crosslinks, mineral fillers or blends.

### REFERENCES

1 Ferry, J. D. in 'Viscoelastic Properties of Polymers', Wiley, New York, 1980

2 Graessley, W. W. in 'Advances in Polymer Science', Springer-Verlag, New York, 1974  
 3 Graessley, W. W. in 'Advances in Polymer Science', Springer-Verlag, New York, 1982  
 4 Flory, J. P. *Br. Polym. J.* 1985, 17, 96  
 5 De Gennes, P. J. in 'Scaling Concepts in Polymer Physics', Cornell University Press, Ithaca, NY, 1979  
 6 Cohen-Addad, J. P. *J. Chem. Phys.* 1974, 60, 2440  
 7 Cohen-Addad, J. P. *J. Physique* 1982, 43, 1509  
 8 English, A. D. *Macromolecules* 1985, 18, 34  
 9 Cohen-Addad, J. P. and Roby, C. *J. Chem. Phys.* 1975, 65, 3091  
 10 Mansfield, P. *Phys. Rev.* 1965, 137A, 961  
 11 Cohen-Addad, J. P. in 'Physics of Finely Divided Matter', (Eds. N. Boccarda and M. Daoud), Springer-Verlag, New York, 1985  
 12 Flory, J. P. in 'Principles of Polymer Chemistry', Cornell University Press, Ithaca, NY, 1953  
 13 Erman, B. and Monnerie, L. *Macromolecules* 1985, 18, 1985  
 14 Cohen-Addad, J. P., Viallat, A. and Huchot, Ph. *Macromolecules* 1987, 20, 2146  
 15 Cohen-Addad, J. P., Domard, M. and Herz, J. *J. Chem. Phys.* 1982, 76, 2744  
 16 Abragam, A. in 'Principles of Nuclear Magnetism', Oxford University Press, London, 1961  
 17 Haeberlen, U. in 'High Resolution NMR in Solids', Academic Press, New York, 1976  
 18 Levitt, M. H. and Freeman, R. *J. Magn. Res.* 1981, 43, 65  
 19 Graessley, W. W. *Adv. Polym. Sci.* 1974, 16, 3

### APPENDIX A

The spin Hamiltonian of the polymer system is written as:

$$\hbar \mathcal{H}_e = \hbar \sum_{k < j} \mathcal{H}_e^{k,j}$$

$\mathcal{H}_e$  concerns all spin-spin interactions  $\mathcal{H}_e^{k,j}$  of proton spins  $k$  and  $j$  located within a given chain segment or on different chain segments.  $\mathcal{H}_e$  is restricted to the adiabatic part of dipole-dipole interactions. Thus:

$$\mathcal{H}_e^{k,j} = \langle (\gamma_p^2 \hbar / 2 d_{k,j}^3) (1 - 3 \cos^2 \theta_{k,j}) \rangle_e (3 I_z^k I_z^j - \mathbf{I}^k \cdot \mathbf{I}^j)$$

The symbol  $\langle \dots \rangle_e$  represents an average over all proton coordinates. This average must account for temporary or permanent stretchings of chain segments. In the present work, attention is mainly focused on properties of spin operators defining  $\mathcal{H}_e^{k,j}$ . It is easily shown that:

$$\mathcal{H}_e^{k,j*} = R \mathcal{H}_e^{k,j} R^{-1} = \langle \dots \rangle_e^{k,j} (3 I_y^k I_y^j - \mathbf{I}^k \cdot \mathbf{I}^j)$$

Then:

$$R^2 \mathcal{H}_e^{k,j} R^{-2} = \langle \dots \rangle_e^{k,j} (3 I_z^k I_z^j - \mathbf{I}^k \cdot \mathbf{I}^j) = \mathcal{H}_e^{k,j}$$

and

$$[\mathcal{H}_e, \mathcal{H}_e^*] \neq 0$$

Furthermore, the commutator  $[\mathcal{H}_e, M_x]$  is expressed as:

$$[\mathcal{H}_e, M_x] = \sum_{k < j, l} \gamma \hbar [\mathcal{H}_e^{k,j}, I_x^l]$$

or:

$$[\mathcal{H}_e, M_x] = \sum_{k < j} 3i \langle \dots \rangle_e^{k,j} \gamma \hbar (I_y^k I_z^j + I_z^k I_y^j)$$

while, the commutator  $[\mathcal{H}_e^*, M_x]$  is expressed as:

$$[\mathcal{H}_e^*, M_x] = - \sum_{k < j} 3i \langle \dots \rangle_e^{k,j} \gamma \hbar (I_y^k I_z^j + I_z^k I_y^j)$$

Therefore:

$$[\mathcal{H}_e, \mathcal{M}_x] = -[\mathcal{H}_e^*, \mathcal{M}_x]$$

### APPENDIX B

The effect of the multiple-pulse sequence proposed in the fourth section upon the transverse magnetization dynamics is analysed in the following way. The description starts at  $t=0$ . At  $t=0_+$  the magnetization  $M_0$  is brought into coincidence with the  $x$ -axis direction (positive values of  $x$ ), in the rotating frame. Then, from  $t=\tau_+$ ,  $p-1$  identical radiofrequency pulses, separated by a constant time interval  $\tau$ , are applied to the spin system. Pulses used to focus the magnetization are ignored because they leave  $\mathcal{H}_e$ ,  $\mathcal{H}_e^*$  and  $\mathcal{M}_x$  operators invariant. Thus, any radiofrequency pulse of the sequence is supposed to induce a  $\frac{1}{2}\pi$  rotation of nuclear spins around the  $x$ -axis.

At  $t=0_+$ , the density matrix operator  $\rho(0_+)$  is set equal to:

$$\rho(0_+) = \mathcal{M}_x$$

A ( $\frac{1}{2}\pi/x$ ) pulse is applied to the spin system at  $t=\tau$ . Then, at  $t=\tau_-$ :

$$\rho(\tau_-) = T_0 \mathcal{M}_x T_0^{-1}$$

and at  $t=\tau_+$ :

$$\rho(\tau_+) = T_1(\tau) \mathcal{M}_x T_1^{-1}(\tau)$$

with

$$T_n(\tau) = e^{i(\alpha_n^* \mathcal{M}_x^{-1})\tau} \quad n=0, 1, 2, \dots$$

The calculation is made in the case where  $\tau_1 = \tau$ .

A second ( $\frac{1}{2}\pi/x$ ) pulse is applied at  $t=2\tau$ . Then, at  $t=2\tau_-$ :

$$\rho(2\tau_-) = T_0(\tau) T_1(\tau) \mathcal{M}_x T_1^{-1}(\tau) T_0^{-1}(\tau)$$

and at  $t=2\tau_+$ :

$$\rho(2\tau_+) = T_1(\tau) T_2(\tau) \mathcal{M}_x T_2^{-1}(\tau) T_1^{-1}(\tau)$$

A  $(p-1)$ th ( $\frac{1}{2}\pi/x$ ) pulse is applied at  $t=(p-1)\tau$ . Then, at  $t=(p-1)\tau_-$ :

$$\rho((p-1)\tau_-) = P_{p-1}(\tau) \mathcal{M}_x P_{p-1}^{-1}(\tau)$$

where:

$$P_{p-1}(\tau) = \prod_{n=0}^{p-2} T_n(\tau)$$

At  $t=(p-1)\tau_+$ :

$$\rho((p-1)\tau_+) = R P_{p-1}(\tau) \mathcal{M}_x P_{p-1}^{-1}(\tau) R^{-1}$$

and at  $t=p\tau$ :

$$\rho(p\tau) = P_p(\tau) \mathcal{M}_x P_p^{-1}(\tau)$$

Clearly,  $P_p(\tau)$  represents a time-ordered exponential operator. It expresses a time integral, from  $t=0$  to  $t=p\tau$ , calculated as a summation over  $p$  short time intervals  $\tau$ :

$$P_p(\tau) \simeq \exp\left(\int_0^{t \simeq p\tau} \mathcal{H}_e^+(t') dt'\right)$$

The above formal expression is written by introducing the convention that  $\mathcal{H}_e^+(t)$  is a time-dependent operator that has alternate expressions  $\mathcal{H}_e$  and  $\mathcal{H}_e^*$  over two successive time intervals  $\tau$ . The operator  $\mathcal{H}_e^+(t)$  does not commute with itself at any time, as is usually the case. Then:

$$M_x^e(t) = \text{Tr}(\rho(p\tau) \mathcal{M}_x) / \text{Tr}(\rho(0) \mathcal{M}_x)$$

The formal exponential operator  $P_p(\tau)$  can be developed as a series expansion of operators. Thus,  $M_x(t)$  is also expressed by a series expansion of functions that can rigorously originate an exponential function. To second order<sup>16</sup>:

$$M_x^e(t) = \exp[C_2(t)]$$

with:

$$C_2(t) = - \int_0^t dt_1 \int_0^{t_1} dt_2 \text{Tr}([\mathcal{H}_e^+(t_1), \mathcal{H}_e^+(t_2), \mathcal{M}_x] \mathcal{M}_x) / \text{Tr}(\mathcal{M}_x^2)$$

Higher-order terms can be neglected by adjusting  $\tau$  to values small enough compared with  $\Delta_r^{-1}$ . The first time integral:

$$I_1(t_1) = \int_0^{t_1} dt_2 [\mathcal{H}_e^+(t_2), \mathcal{M}_x]$$

is calculated from a summation over small time intervals  $\tau$ . For  $t_1=2l\tau$ , alternate signs of the commutator give  $I_1(2l\tau)=0$ . For  $t_1=(2l+1)\tau$ , alternate signs give:

$$I_1(t_1) = [\mathcal{H}_e, \mathcal{M}_x] \tau$$

The second time integral:

$$I_2(t) = \int_0^t dt_1 [\mathcal{M}_x, \mathcal{H}_e^+(t_1)] I_1(t_1)$$

is also calculated from a summation over small time intervals  $\tau$ . For  $t=2l'\tau$ :

$$I_2(t) = l'\tau [\mathcal{M}_x, \mathcal{H}_e] [\mathcal{H}_e, \mathcal{M}_x] \tau$$

For  $t=(2l'+1)\tau$ ,  $I_2(t)$  is also equal to  $-l'\tau^2 [\mathcal{M}_x, \mathcal{H}_e]^2$ . Therefore:

$$C_2(t) = -M_x^e \tau t / 2$$

Consequently, the relaxation function is expressed as a pure exponential time function:

$$M_x(t) = e^{-M_x^e \tau t / 2}$$

The time interval  $\tau$  is twice the time interval separating two consecutive ( $\frac{1}{2}\pi/x$ ) and  $(\pi/x)$  pulses.